MODELLING OF THE PERMEABILITY OF NON-CRIMP-STITCHED FABRICS

T. Staffan Lundström and Markus Zetterberg

Department of Polymeric Materials
Chalmers University of Technology
SE-912 96 Gothenburg, Sweden

INTRODUCTION

It is well established that the flow of resin through the reinforcing fibres during the manufacturing of composites by liquid moulding processes follows Darcy's law. This implies that the fibre reinforcements can be characterised by its permeability through measurements or by the usage of permeability models based on, for instance, the detailed fibre geometry. The fibre reinforcements used for composites manufactured by liquid moulding processes are, in most cases, formed by fibres which are gathered in bundles. This results in two types of flow: A microscale flow within the fibre bundles and a mesoscale flow between the bundles. Typical length scales for the two types of flow are < 10 μm and > 100 μm, respectively. It has been shown that the relation between the microflow and mesoflow is important for flow front phenomena such as void formation while a number of studies have indicated that the overall flow rate through the material is, to a large extent, set by the mesoflow; cf., for instance, [1, 2]. This is easily understood by noticing that the volumetric flow rate per unit area is proportional to the square of the characteristic length scale in Poiseuille flow. Hence, the flow rate per unit area on the mesoscale is as a rule of thumb, one hundred times higher or more than it is on the microscale as long as the geometry on the two scales is principally the same.

A number of models have been presented that consider the flow on the microscale. Of particular interest are the models that are aimed at high fibre volume fractions, i.e. when the fibres are close to each other. Two such models were presented by Gebart [3] for flow along and perpendicular to a perfect arrangement of fibres. Both these models are expressed in terms of the fibre volume fraction, V_f and the fibre radius R according to:

$$K_{//} = \frac{8}{c}\frac{(1-V_f)^3}{V_f^2}R^2, \quad K_{\perp} = C\left(\sqrt{\frac{V_{f\max}}{V_f}}-1\right)^{5/2}R^2 \qquad \text{(1a-b)}$$

The maximum fibre volume fraction V_{fmax} and the two constants c and C are dependent on the actual fibre arrangements, quadratic or hexagonal. The first of these equations are based on the hydraulic radius and can be recognized as the often-used Kozeny-Carman Equation. An alternative model for flow perpendicular to highly packed assemblies of fibres has been presented in [4]. A direct comparison to (1b) yields a small deviation that decreases as the fibre volume fraction approaches the maximum. The close similarity between (1a-b) and other equations presented in the literature results in our using (1a-b) for the flow through the fibre bundles with some confidence. It is, however, clear that deviations in the real fibre geometry from the perfect arrangements assumed in (1a-b) may, to some extent change the results [5].

The interest in the flow on the two scales has increased the recent few years [1, 2, 6-9]. In particular Shih and Lee [8] have proposed a parallel permeability model for flow through bi-directional stitched fabrics. The flow through the fibre bundles were set by models for flow along and perpendicular to perfect arrays of fibres and the flow between the bundles by the Kozeny-Carman equation. In [9] the flow between the bundles were modelled by solving the Stoke's equations for flow through a pipe and for flow between two parallel plates. It is assumed that the velocity of the fluid at the permeable boundary is equal to the velocity within the porous media. In reality there will be a boundary layer within the porous media in which the velocity is higher than the one set by Darcy's law. This boundary layer flow results in a higher velocity at the boundary as compared to the Darcy velocity and hence a comparably larger volumetric flow rate through both the porous media and the channels [10, 11].

The focus will here be set on the permeability of non-crimp stitched fabrics. These fabrics have a fairly simple geometry as long as they are unloaded. But as will appear in this paper the geometry may considerably change during compaction. At first, a model for the flow will be derived which is based on a simplified model for the compaction. The model will then be applied on two fabrics for the permeability of which is measured. The input parameters to the model are obtained from micrographs of the unloaded samples and from cross-sections of the fabrics at the fibre volume fractions considered. Finally, the results are discussed.

MODELLING

The unloaded model geometry is built up of straight fibre bundles. The bundles are organised in layers each consisting of one row of parallel fibre bundles. In the following layer the bundles are directed 90 degrees to the previous layer, given a structure as shown in Fig. 1. The bundles are allowed to have a certain horizontal distribution in size and placement and each row are arbitrarily placed in the plane. The spaces formed between the bundles are the interbundle channels. Their geometry is obviously set by the shape and placement of the bundles. Five assumptions on the geometry will now be introduced some of which will be relaxed in the second step of the model. First of all it is assumed that the bundles will attain a rectangular shape as the fabric is compressed to higher fibre volume fractions, i.e. such as are considered here. This implies that the interbundle channels also become rectangular shaped which is a fairly good approximation for the fabric studied as exemplified in Fig. 2. Secondly, it is assumed that the fibrebundles have a uniform cross-sectional area in the flow direction and that the fibres in the fibre bundles are perfectly aligned with the flow. This implies that a fluid particle that has entered an interbundle channel or a fibre bundle directed along the flow will stay there. The third assumption is that any influence from the stitching material is neglected. Furthermore, it is assumed that the compression of the bundles will not influence the width of the bundles and consequently not the width of the interbundle channels either. Finally, the height of the interbundle channel is set by the height of each layer. Hence, all the bundles perpendicular to the plane will remain straight during compression and every interbundle channel will have the same height.

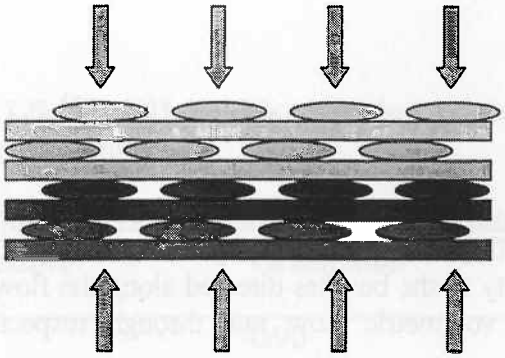

Fig. 1. Initial model geometry

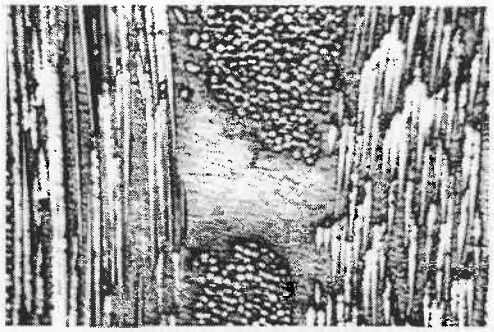

Fig. 2. Example of channel cross-sectional area.

The main assumptions for the flow equations are that the fluid is Newtonian and that it is flowing at low Reynolds number, (much less than 1). It will, furthermore, be assumed that the velocity at the boundary between the fibre bundles and the channels is equal to the Darcy velocity within the bundles. The permeability of one layer with the fibres along the flow may then be expressed as [12]:

$$K_{along} = \frac{\sum_{n=1}^{m} K_c^n A_c^n + \sum_{n=1}^{m} K_b^n A_b^n}{\sum_{n=1}^{m} A_c^n + \sum_{n=1}^{m} A_b^n} \tag{2}$$

where A is the area cross to the flow and the indices m, n, c and b denote, the number of bundles and channels, the nth bundle or channel, bundle and channel, respectively. Regarding the layers with the fibres cross to the flow, the fluid will alternatively move within the fibre bundles and between the bundles. Hence the permeability is given from [12]:

$$K_{perp} = \frac{L}{\sum_{n=1}^{m} \frac{w_c^n}{K_c^n} + \sum_{n=1}^{m} \frac{w_b^n}{K_b^n}} \approx \frac{L}{\sum_{n=1}^{m} \frac{w_b^n}{K_b^n}} \tag{3}$$

where L is the length in the flow direction and w the width of the bundles and the channels in the flow direction. The second expression is obtained by assuming that the permeability in the bundles is much lower than that of the channels at the same time as the width of the channels is in the same range as the width of the bundle. The total permeability is now given from:

$$K = \sum_{j=1}^{i} K_{along}^{j} + \sum_{l=1}^{k} K_{perp}^{l} = \sum_{j=1}^{i} \left(\frac{\sum_{n=1}^{m} K_c^n A_c^n + K_b^{along} A_b^{tot}}{A_c^{tot} + A_b^{tot}} \right)^j + \sum_{l=1}^{k} \left(\frac{L}{w_b^{tot}} K_b^{cross} \right)^l \tag{4}$$

with the assumption that all bundles have the same permeability (although different along and cross to the flow). The indices i, j, k and l are the summation parameters for the layers directed along and cross to the flow direction. The permeability for flow along and cross to the fibre

bundles is here approximated with (1a-b) by setting c equal to 53, C equal to $16/\left(9\pi\sqrt{2}\right)$ and V_{fmax} equal to $\pi/\left(2\sqrt{3}\right)$ (hexagonal pattern).

It remains now to find an expression for the permeability of the channels. By setting the velocity at the boundaries of these channels to the Darcy velocity of the bundles directed along the flow and by the previously presented approximations the volumetric flow rate through respectively interbundle channel is the following:

$$Q^n = \frac{\Delta p}{L}\frac{w_n^4}{\mu}\left[\frac{16}{\pi^5}\sum_{\alpha=0}^{\infty}\frac{1}{\beta^5}\frac{\left(e^{\beta\pi\frac{h_n}{w_n}}-1\right)}{e^{\beta\pi\frac{h_n}{w_n}}+1}+\frac{1}{12}\frac{h_n}{w_n}\right]+Vh_n w_n \tag{5}$$

where V is the Darcy velocity at the boundary between the channel and the bundle. Furthermore, h and w are the height and width of the rectangular shaped interbundle channels, respectively and $\beta = (2\alpha+1)$. By usage of Darcy's law and (5), the permeability of one interbundle channels may be expressed as:

$$K^n = \frac{w_n^3}{h_n}\left[\frac{16}{\pi^5}\sum_{\alpha=0}^{\infty}\frac{1}{\beta^5}\frac{\left(e^{\beta\pi\frac{h_n}{w_n}}-1\right)}{e^{\beta\pi\frac{h_n}{w_n}}+1}+\frac{1}{12}\frac{h_n}{w_n}\right]+\frac{K_b^{along}}{\left(1-V_{fb}\right)} \tag{6}$$

The permeability of the whole stack is then obtained from (1a-b), (4) and (6) if the geometrical parameters included can be determined.

MATERIALS AND EXPERIMENTAL EQUIPMENT

The materials utilised to test the model are two Ahlström non-crimp-stitched fabrics; cf. Table 1. The second fabric differs from the first by having less bundles in each direction. This implies that the bundles, on the average, are larger for the second fabric. The number of bundles is also different in the two directions of the fabrics giving the same implication. The stitching material furthermore sets the geometry of the fabrics. As a consequence of the method of production the interbundle channels in the production direction are in most cases free from fibres while in the perpendicular direction the fibres often goes from one bundle to the other and hence crossing the interbundle channels; cf. Fig. 3. The fabrics were studied at three fibre volume fractions namely, 46.9 %,

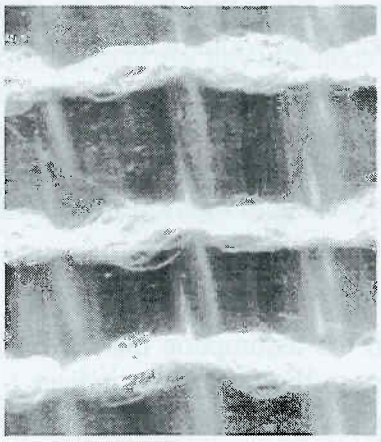

Fig 3. Example of fibres crossing the channels

52.7 % and 60.3 %. This results in a height of each ply of fabric of 0.75 mm, 0.67 mm and 0.58 mm respectively.

Table 1. Data on the Ahlström fabrics utilised.

Number	Orientation	Surface density (g/m^2)	Number of bundles per meter
1	0/90	450/450	260/360
2	0/90	450/450	240/280

The permeability equipment used is described in detail in [13]. It is a parallel flow cell and the permeability is obtained from saturated samples. The permeability is measured along and perpendicular to the production direction of the fabric at the three fibre volume fractions considered and for three samples in each case. It is here assumed that the measurements are carried out in the principal directions of the fabrics and hence, the one-dimensional form of Darcy's law is used to derive the permeability values.

In addition to these measurements some composite plates were manufactured at the two highest fibre volume fractions. From these plates cross-sections were cut and polished so that the actual shape of the interbundle channels of a deformed fabric could be studied. This was carried out by means of an optical microscope connected to an image analysis system. The geometry of a single unloaded ply was measured with the same apparatus.

COMPARISON BETWEEN THE MODEL AND THE EXPERIMENTAL RESULTS

To the model proposed five input parameters are required. They are the following: 1) the fibre volume fraction within the bundles, 2) the fibre radius, 3) the number of bundles and channels per unit width and unit length and 4-5) the height and the width of the interbundle channels. It will turn out that the actual fibre radius and the fibre volume fraction within the fibre bundle is of less importance as long as the radius is small enough and the fibre volume fraction large enough. Hence, the following values on these parameters will be used: $V_{fb} = 75\%$ and $R = 7$ mm. The rest of the parameters will be obtained in two ways. Firstly by studies of unloaded fabrics and secondly by studies of cross-sections of compressed fibre reinforcements.

In the unloaded case the width of about 150 channels in each direction and for each reinforcement were derived from samples cut from the fabric while the channel height was approximated by the height of each layer in the compressed state. Not surprisingly this approximation overestimate the permeability as shown in Table 2. It can, however, be stated that the model, with these input parameters, works at its best at low fibre volume fractions and for flow in the production direction of fabric 1. The large deviation at higher fibre volume fractions indicates that the geometry of the fibre bundles does change differently to what is assumed. Two assumptions were that the height of the channels was set by the height of one layer and that the width of the channels could be approximated by their width at the undeformed state. A more accurate but certainly more time-consuming way to get the width and height of the interbundle channels is to study polished cross-sections of composite laminates made at the fibre volume fractions of interest. This is done here for some of the cases. As appears from Table 2 the accuracy of the results becomes much better. However at high fibre volume fractions and for the second fabric the results are still not satisfying.

The microscopic studies revealed some feature of the reinforcements. First of all and not very surprisingly the bundles are not perfectly aligned to each other. Secondly the cross-sectional area of the bundles in the production direction of the fabric are brick-like as assumed in the model while the ones in the perpendicular direction are more lens-shaped. The consequence of the lens-shape is that the perpendicular bundles are more easily compressed into the channels pointing perpendicular to the production direction. It is furthermore observed that the stitching may certainly influence the geometry of the fabric. However it is not clear how much this will affect the permeability.

Table 2. Comparison between model and measured permeability.

Material	Fibre volume fraction (%)	Direction	Ratio between the permeability derived from the model and the measured permeability	
			Unloaded case	Loaded case
Fabric 1	46.9	Production	1.8	-
		Perpendicular	2.7	-
	52.7	Production	3.0	1.2
		Perpendicular	7.0	1.3
	60.3	Production	9.2	2.9
		Perpendicular	13.3	-
Fabric 2	46.9	Production	3.6	-
		Perpendicular	2.2	-
	52.7	Production	6.9	2.1
		Perpendicular	5.5	4,7
	60.3	Production	19.1	2.7
		Perpendicular	10.9	-

DISCUSSIONS

A model for flow through a non-crimp-stitched fabric has here been presented. The aim with the model is to understand the flow through such fabrics so that high permeable reinforcements can be developed. The model is two-dimensional and based on Darcy's law within the bundles and Stoke's flow between them. The model compares well with experimental results at certain events but less for other cases. With proper input data the model predicts the permeability of one of the test fabrics in a nice way without any fitting parameters. This indicates that the model is not totally incorrect. However, in all cases the model overrates the permeability. A probable reason for this is that the model is two-dimensional while the fabric has a three dimensional structure. It was, for instance, observed that the width of the interbundle channels varies quite much in the flow direction of the fabric. This is a result of the bundles not being completely straight and hence for every converging channel there is often a diverging channel nearby. Another observation was that in some cases the perpendicular bundles were compressed into the interbundle channels. One fact that still gives the two dimensional approach some validity is that the channels are interconnected and, hence, if there is a constriction in one channel the fluid particles may move into a neighbouring channel. This redistribution of the fluid may take place on much smaller length scales than the length scale for the change in the channel width. However, in the case of constrictions due to the perpendicular fibre bundles the length scale for the fluid distribution and the change in the channel height may be the same. Hence, the development of a three-dimensional model would be of greatest interest. Another area of improvement is the boundary conditions at the walls of the conduit. The results in, for instance, [10] indicates that the velocity at the boundaries is

somewhat larger than what has been assumed here. It is also clear that the compression model should be improved in such a way that it takes into account the deformation of the fibre bundles into the interbundle channels. Such a deformation can certainly affect the permeability of the fabrics considered.

ACKNOWLEDGEMENT

The authors wish to thank Prof. Staffan Toll for fruitful discussions, Birgitta Johansson for doing some of the measurements and Ahlström Glassfibre OY, Mikkeli Plant for the materials.

REFERENCES

1. Papathanasiou, T.D., *A structure-orientated micromechanical model for viscous flow through square arrays of fibres.* Composites Science and Technology, 1996. **56**: p. 1055-1069.
2. Binétruy, C., Hilaire, B., Pabiot, J., *The interactions between flows occurring inside and outside fabric tows during RTM.* Composite Science and Technology, 1997. **57**: p. 587-596.
3. Gebart, B.R., *Permeability of unidirectional reinforcements for RTM.* Journal of Composite Materials, 1992. **26**: p. 1100-1133.
4. Sangani, A.S., Acrivos, A., *Slow flow past periodic arrays of cylinders with application to heat transfer.* International journal of Multiphase flow, 1982. **8**(3): p. 193-206.
5. Lundström, T.S., Gebart, B.R., *Effect of perturbation of fibre architecture on permeability inside fibre tows.* Journal of Composite Materials, 1995. **29**: p. 424-443.
6. Phelan Jr., F.R., Spaid, M.A.A. *Modelling of unsaturated flow dynamics in composite processing.* in *Fifth international Conference on Automated Composites.* 1997. Glasgow, UK.
7. Pearce, N.R.L., Summerscales, J. *The modification of fabric architecture to improve the processing of continuous fibre reinforced composites manufactured by RTM.* in *FRC '98.* 1998. Newcastle upon Tyne, England.
8. Shih, C.-H., Lee, L.J., *Effect of fiber architecture on permeability in liquid composite molding.* Polymer Composites, 1998. **19**(5): p. 626-639.
9. Kolodziej, J.A., Dziecilak, R., Konczak, Z., *Permeability tensor for heterogeneous porous medium of fibre type.* Transport in porous media, 1998. **32**: p. 1-99.
10. Beavers, G.S., Sparrow, E.M., Magnuson, R.A., *Experiments on Coupled Parallel Flows in a Channel and a Bounding Porous Medium.* Journal of Basic Engineering, 1970. **92D**: p. 843-848.
11. Gupte, S.K., Advani, S.G., *Flow near a permeable boundary of an aligned fiber preform: An experimental investigation using laser doppler anemometry.* Polymer Composites, 1997. **18**(1): p. 114-124.
12. Bear, J., *Dynamics of fluids in porous media.* 1972: Dover Publications Inc.
13. Lundström, T.S., Toll, S., *Measurement of the 3D permeability tensor of stationary fibre beds under a uniaxial compression load.* To be published, .